REGULAR ARTICLE

blood advances

Dynamins 2 and 3 control the migration of human megakaryocytes by regulating CXCR4 surface expression and ITGB1 activity

Praveen K. Suraneni,[1] Seth J. Corey,[2-5] Michael J. Hession,[2] Rameez Ishaq,[6-9] Arinola Awomolo,[2] Shirin Hasan,[1] Chirag Shah,[1,10] Hui Liu,[11] Amittha Wickrema,[11] Najet Debili,[6-8] John D. Crispino,[1] Elizabeth A. Eklund,[1] and Yolande Chen[1,2]

[1]Department of Medicine and [2]Department of Pediatrics, Northwestern University School of Medicine, Chicago, IL; [3]Department of Pediatrics, [4]Department of Microbiology/Immunology, and [5]Department of Human and Molecular Genetics, Virginia Commonwealth University, Richmond, VA; [6]Unité mixte de recherche (UMR) 1170, INSERM, Equipe labellisée, Ligue Nationale contre le Cancer, Villejuif, France; [7]UMR 1170, INSERM, Université Paris-Saclay, Villejuif, France; [8]UMR 1170, INSERM, Institut Gustave Roussy, Villejuif, France; [9]Institut Universitaire, Hématologie, Université Paris 7 Diderot, Paris, France; [10]MilliporeSigma, Burlington, MA; and [11]Department of Medicine, University of Chicago, Chicago, IL

Key Points

- DNMs promote the directional migration of MKs by affecting CXCR4 surface expression, ITGB1 activity, and RhoA activity.
- DNM-induced migration and cytoskeletal-membrane changes enable spatial control of proplatelet formation in the proper niche.

Megakaryocyte (MK) migration from the bone marrow periosteal niche toward the vascular niche is a prerequisite for proplatelet extension and release into the circulation. The mechanism for this highly coordinated process is poorly understood. Here we show that dynasore (DNSR), a small-molecule inhibitor of dynamins (DNMs), or short hairpin RNA knockdown of DNM2 and DNM3 impairs directional migration in a human MK cell line or MKs derived from cultured $CD34^+$ cells. Because cell migration requires actin cytoskeletal rearrangements, we measured actin polymerization and the activity of cytoskeleton regulator RhoA and found them to be decreased after inhibition of DNM2 and DNM3. Because SDF-1α is important for hematopoiesis, we studied the expression of its receptor CXCR4 in DNSR-treated cells. CXCR4 expression on the cell surface was increased, at least partially because of slower endocytosis and internalization after SDF-1α treatment. Combined inhibition of DNM2 and DNM3 or forced expression of dominant-negative Dnm2-K44A or GTPase-defective DNM3 diminished β1 integrin (ITGB1) activity. DNSR-treated MKs showed an abnormally clustered staining pattern of Rab11, a marker of recycling endosomes. This suggests decreased recruitment of the recycling pathway in DNSR-treated cells. Altogether, we show that the GTPase activity of DNMs, which governs endocytosis and regulates cell receptor trafficking, exerts control on MK migration toward SDF-1α gradients, such as those originating from the vascular niche. DNMs play a critical role in MKs by triggering membrane-cytoskeleton rearrangements downstream of CXCR4 and integrins.

Introduction

A critical step in megakaryocytopoiesis is the migration of megakaryocytes (MKs) from the periosteal/osteoblastic bone marrow (BM) niche, where early-stage MK progenitors expand and reside, toward the vicinity of the BM sinusoid blood vessels.[1-11] Interactions with the microenvironment also enable mechanosensory signaling transduction within the MKs.[12-14] Once localized in the proximity of marrow sinusoids, MKs are surrounded by a different environment and can either migrate or extend proplatelets through the endothelial barrier. Previous studies have reported that MKs migrate toward an SDF-1α gradient; however, the intracellular processes that regulate MK migration are not well known[9,11,15-17] and constitute a gap in our knowledge.

Submitted 4 June 2018; accepted 4 November 2018. DOI 10.1182/bloodadvances.2018021923.

The full-text version of this article contains a data supplement.

We previously reported that mice lacking CIP4 (Cdc42-interacting protein 4), an F-BAR protein involved in endocytotic vesicle formation, display thrombocytopenia associated with defects in membrane invagination.[18] The SH3 domain of an F-BAR protein can interact with a proline-rich region in dynamins (DNMs), a family of proteins with GTPase activity.[19] DNMs are best known as facilitators of membrane twisting that leads to endocytic vesicle release. Whereas DNM2 is ubiquitous, DNM3 is expressed in the nervous system, lung, heart, testis,[19] pancreatic β cells,[20] and MKs.[21]

Both DNM2 and DNM3 are expressed in human MKs. Some *DNM2* mutations are associated with platelet counts in the lower range.[22] In large human populations, a genome-wide association study found that a *DNM3* variant transcript is strongly predictive of mean platelet volume.[23,24] This suggests a role for DNMs in human platelet biogenesis, but the exact mechanism has not been established. Redundancy between DNM isoforms may exist and has been documented in the cases of murine Dnm1 and Dnm3.[25] The extent of redundancy between human DNM2 and DNM3 is unknown, but it may explain why constitutive *DNM2* mutations in Charcot-Mary-Tooth patients have minor effects on platelet counts.[22,25] In murine MKs, where Dnm2 predominates and the role of Dnm3 seems minimal,[26] loss of *Dnm2* yields severe macrothrombocytopenia, MK extramedullary hyperplasia, proliferation of immature MKs, and myelofibrosis.[27] This phenotype has been hypothesized to result from defective endocytosis of the thrombopoietin (TPO) receptor. However, because DNMs regulate endocytosis and intracellular trafficking, the effects of DNM loss may be wider.

While investigating potential effects of DNM inhibition in MKs, we noticed that MKs exhibit a striking migration defect, and we set out to investigate the role of DNMs in MK migration. DNMs can control the migration of cancer cells,[28-31] but the effect of DNMs on the interaction of MKs with the matrix and MK migration is largely unknown. Consistent with their membrane remodeling properties and capabilities in controlling actin polymerization, DNMs have been described as regulating cell surface receptor trafficking[32] and Rho GTPase activity,[31,33,34] both relevant to cell motility. Therefore, we sought to determine how DNMs control MK directional migration via effects on cell surface receptors upstream of membrane-cytoskeletal rearrangements. Particular attention was given to β1 integrin (ITGB1) and CXCR4, which respectively drive hematopoietic cell migration and migration toward marrow sinusoids.[6,35]

Methods

Cell lines and MK cultures

The megakaryocytic cell lines CHRF-288-11 (hereafter CHRF) and MEG-01 were a gift from William Miller at Northwestern University and were cultured in Iscove modified Dulbecco medium (Gibco; ThermoFisher Scientific, Waltham, MA) with 10% fetal bovine serum (Hyclone; GE Healthcare, Chicago, IL) and permeability surface area product for glucose (Gibco). In some cases, puromycin or G418 (Gibco) was added. Cultures were kept in humidified incubators at 37°C with 5% carbon dioxide. Human CD34-selected cord blood cells (StemCell Technologies, Vancouver, BC, Canada) were cultured in SFEM-II (StemCell Technologies) with human cytokines (PeproTech, Rocky Hill, NJ; 50 ng/mL of TPO, 30 ng/mL of stem cell factor, 10 ng/mL of interleukin-3, and 10 ng/mL of FLT3 ligand for 48 hours, then TPO and stem cell factor until day 6, then TPO only) to allow megakaryocytic differentiation. The purity of MK-enriched populations was assessed by flow cytometry CD41 expression, and all samples were found to have >80% to 85% cells expressing CD41.

Fluorescence anisotropy was performed as previously described.[18] Briefly, cells were labeled with 1 μM of 1-(4-(trimethylamino) phenyl)-6-phenylhexa-1,3,5-triene (TMA-DPH; Invitrogen, Carlsbad, CA) at 37°C for 10 minutes and stimulated with phorbol 12-myristate 13-acetate (PMA; Sigma, St Louis, MO). End point readings were taken to detect changes in plasma membrane fluidity. Fluorescence anisotropy (*r*) values were recorded using a Spectramax M5 microplate reader at the Northwestern Institute for BioNanotechnology.

Western blot analysis

Western blots were performed as previously described.[18] Antibodies are listed in the supplemental Materials and methods.

Flow cytometry analysis, cell sorting, immunofluorescence, and confocal imaging

Flow cytometry was performed as previously described.[18,36] F-actin polymerization was quantified by flow cytometry as described by Riviere et al,[3] but without additional SDF-1α or fibronectin (FN). Briefly, MKs were fixed with 0.5% paraformaldehyde, washed, permeabilized in 0.01% Triton-X, and incubated with fluorochrome-conjugated phalloidin and anti-CD41.

Antibodies are listed in the supplemental Methods. 4′,6-diamidino-2-phenylindole (DAPI) was purchased from Invitrogen (#D1306). Data were acquired on a BD LSR/Fortessa 6-Laser Analyzer and analyzed with FlowJo (Ashland, OR), and cell sorting was performed on a FACSAria cell sorter at the Northwestern Core Facility.

Imagestream (MilliporeSigma, Burlington, MA) data were acquired at the University of Chicago Flow Cytometry Facility and analyzed using IDEAS software (MilliporeSigma). Immunofluorescence analysis was performed on treated and untreated MKs as previously described[18] and per supplemental Methods. Images were obtained using a Nikon A1R+ confocal microscope under a ×60 or ×100 Plan-Apochromat oil immersion lens, a DeltaVision OMX super-resolution fluorescent microscope under a ×63 objective, a Nikon Biostation (×20 objective), or a Nikon Eclipse TS100 (×40 objective). Quantification was performed with ImageJ (National Institutes of Health, Bethesda, MD).

Short hairpin RNA and DNM constructs

Lentiviruses were produced as previously described,[36] and MKs were transduced at days 5 and 6 of culture. Details are provided in the supplemental Methods.

Complementary DNA synthesis

Total RNA was extracted using Trizol; complementary DNA was synthesized with the iScript kit (BioRad, Hercules, CA). Polymerase chain reaction was performed on a BioRad iCycler.

Migration assays

CHRF cell chemotaxis assays were performed as previously described,[37] with some modifications. Briefly, control and short hairpin DNM2 (shDNM2)– and shDNM3-treated cells were allowed to migrate in μ–Slide chemotaxis slides (#80326; IBIDI, Madison, WI) precoated with 25 μg/mL of FN. The cells were starved for 6 hours in a low-serum medium (RPMI [Gibco] with 0.5% fetal

bovine serum), followed by replacement with full RPMI medium. The chemotaxis gradient was established by introducing SDF-1α at 150 ng/mL (PeproTech) through 1 of the ports, and cell migration was recorded on an inverted Nikon Biostation microscope with a 37°C incubator and 5% carbon dioxide for 12 hours with frames taken every 10 minutes. Cell trajectory analysis was performed as described previously,[38] with modifications using the IBIDI cell tracker software and ImageJ. Migration directionality was computed as the ratio of displacement/path length from trajectory analysis. MK migration was studied in transwell migration assays using 8-μm pore inserts (Costar; Sigma Aldrich) toward an SDF-1α gradient (PeproTech; 100 ng/mL in the lower compartment) for 5 hours at 37°C, as previously described.[39]

Rho GTPase activity assays

RhoA, Rac, and Cdc42 activation were measured with G-LISA kits from Cytoskeleton (#BK124-S, #BK128-S, and #BK127-S; Denver, CO). Proplatelet formation (PPF) studies were carried as previously described.[40] Other chemicals and reagents used included: dimethyl sulfoxide (#D8418; Sigma), dynasore (DNSR; #7693; Sigma) used at 80 μM for 36 hours unless stated otherwise, and FN (#F1141; Sigma) used at 25 μg/mL.

Statistical analysis was performed with GraphPad software (La Jolla, CA), using a Student *t* test to compare the mean ± standard error of the mean, with the assumption of normal distribution, unless mentioned otherwise, or Mann-Whitney *U* test, with $P < .05$ considered significant.

Results

DNM2 and DNM3 are expressed in human MKs, and their functions overlap

Because human MKs possess both DNM2 and DNM3,[21,41] we asked whether DNM2 and DNM3 are spatially and functionally redundant. Using super-resolution microscopy, we did not observe colocalization of DNM2 and DNM3, but both displayed a dot pattern throughout the whole cytoplasm (Figure 1A). Thus, super-resolution imaging suggested that the isoforms could operate distinctly from each other.

To perform functional testing, we knocked down DNM2 and/or DNM3 with shRNAs in the megakaryocytic CHRF cell line and confirmed decreased protein expression by western blot. DNM2 migrated as a single band as expected. However, using an antibody specific for the human form, DNM3 migrated as 2 bands: 1 at ~90 kDa corresponding to the classical isoform, and another at ~75 kDa corresponding to a previously described shorter alternate isoform, derived from an alternative *DNM3* transcript (Figure 1B), and a putative determinant of MPV.[23,24] Notably, the shRNA specific for *DNM3* produced a decrease in the expression of both bands, suggesting that both bands correspond to DNM3. We observed that this second isoform is also present in human primary MKs (Figure 1C).

We next examined the behavior of cells with DNM2 and/or DNM3 knockdown. We first measured the plasma membrane fluorescence anisotropy in response to PMA. Anisotropy was recorded on cells labeled with TMA-DPH, a molecular probe that localizes specifically in the plasma membrane. Anisotropy values (*r*) correlate with membrane stabilization and are inversely proportional to membrane fluidity.[42] Treatment with PMA induces widespread membrane rearrangements, and endocytosis of invaginated membrane decreases the *r* value.

The *r* value drop (signifying increased membrane fluidity/destabilization) tended to be lesser in cells with individual knockdown than in control cells, but the difference in value in controls became significant when both isoforms were knocked down (Figure 1D; supplemental Figure 1A-C). To confirm this on a larger cellular scale, we studied changes in membrane lipid raft staining pattern, using fluorochrome-conjugated cholera-toxin B (CTXB) and Imagestream. After lipid raft staining, the cells can be categorized into a low-contour (dot-like) pattern group, high-contour (circumferential membrane staining) pattern group, intermediate-low–contour pattern group, and intermediate-contour pattern group (supplemental Figure 1D). After treatment with SDF-1α, control CHRF cells demonstrated an increased signal within the intermediate-contour staining group, whereas this response in CHRF cells with shDNM2 and shDNM3 double knockdown was diminished (supplemental Figure 1D). This finding corroborates the fact that dynamic changes in response to stimulus are diminished in the plasma membrane of shDNM2 and shDNM3 knockdown cells.

Overall, these results suggest that the functions of DNM2 and DNM3 are partially additive and partially overlap. Of note, DNSR treatment of primary MKs resulted in diminished response in the high-contour pattern group after SDF-1α treatment and staining of membrane lipid rafts (supplemental Figure 1E). In additional experiments detailed in "DNM activity regulates actin polymerization, RhoA activation, and CXCR4 surface expression in human MKs" and "DNMs regulate surface integrins in MKs," shRNA targeting of both DNMs led to stronger effects than targeting each individually. Therefore, when performing the subsequent functional assays on primary MKs, we used the DNM inhibitor DNSR, which inhibits the GTPase activity of all DNMs. Mortality of DNSR-treated MKs was assessed by DAPI cell staining in flow cytometry experiments and averaged 7.5% in DNSR cells vs 4% in control cells, in excess of 3.5% compared with vehicle-treated cells (supplemental Figure 1F).

DNM inhibition impairs MK migration

We first studied whether DNM affects migration in CHRF cells. To limit the potential rescue of 1 isoform by the other, we knocked down both in the CHRF cells (shDNM2 and shDNM3 CHRF cells). We used a commercially available microfluidics-based μ-chamber. FN[43] was selected as a substrate rather than collagen, because MKs notably show little migration on collagen.[9] Control cells (treated with nontargeting shRNAs) and shDNM2 and shDNM3 cells were left to migrate.

Cell positions were tracked by time-lapse imaging. Without SDF-1α, no difference between control and shDNM2 and shDNM3 CHRF cells was found, because both types of cells displayed random migration (supplemental Figure 2A). When cells were left to migrate toward an SDF-1α gradient, we found that shDNM2 and shDNM3 CHRF cells had reduced directional migration (Figure 2A-B; supplemental Videos 1 and 2). We then studied the migration of primary human MKs, which we cultured by differentiating cord blood–derived $CD34^+$ cells (Figure 2C). During optimization trials using this microfluidics-based system, we observed that the primary MKs did not survive in sufficient numbers to allow for meaningful data collection. Therefore, we used the more traditional transwell migration assay toward an SDF-1α gradient. We found that DNSR led to a 45% decrease in primary MK migration (Figure 2D; supplemental Figure 2B).

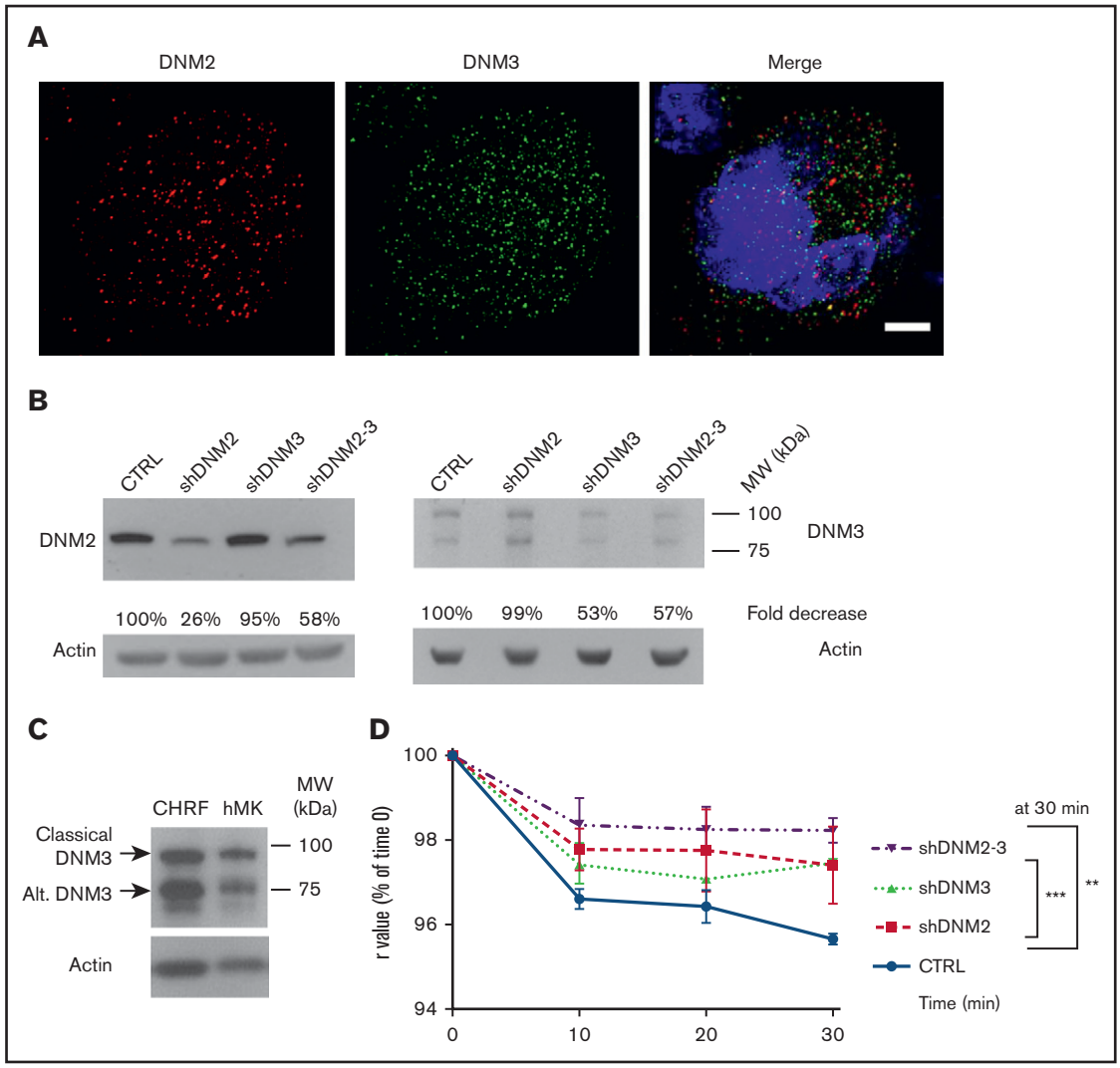

Figure 1. DNM2 and DNM3 are expressed in human MKs and modify plasma membrane anisotropy. (A) OMX super-resolution microscopy image of DNM2 (red) and DNM3 (green) staining in human MKs; original magnification, 63× objective. Twenty-five or more primary MKs were analyzed by confocal immunofluorescence. Here shown are OMX super-resolution microscopy images for illustration purposes. DNM2 specks are distinct from the DNM3 dotted staining, and both are distributed throughout the cytoplasm. Blue stains for the nucleus. Scale bar represents 2 μm. (B) Western blot (WB) of DNM2 and DNM3 and efficiency of their knockdown in CHRF cells. DNM2 presented as a single band in the megakaryocytic CHRF cells, whereas DNM3 migrated as 2 bands: a band at ~90 kDa corresponding to the classical transcript, along with a shorter band, corresponding to an alternate DNM3 transcript (~75 kDa). The fold change of DNM expression in shRNA-induced knockdown, compared with control (CTRL) cells (nontarget CTRL shRNA), is indicated as a percentage of CTRL. (C) WB staining of DNM3 in CHRF cells and MKs. The presence of the alternate (Alt) DNM3 band (arrow) is confirmed in primary human MKs (hMKs) differentiated from cord blood CD34 cells. (D) Plasma membrane fluorescence anisotropy measurement in CHRF cells with DNM2 and DNM3 knockdown. The measurement of plasma membrane fluorescence anisotropy values (*r*) in response to activation by PMA (1 μM) indicated a trend for decreased membrane fluidity, deformation, and remodeling for cells with single DNM knockdown and showed significant difference from CTRL for cells with double shDNM2 and shDNM3 knockdown (at 30 minutes). The stronger effect with double knockdown suggested that the actions of DNM2 and DNM3 overlap to a certain degree. Error bars indicate standard errors of the mean of ≥3 independent experiments. $^{**}P \leq .01$, $^{***}P \leq .001$. MW, molecular weight.

In mice, Dnm2 is crucial to megakaryopoiesis,[27] whereas Dnm3 is minimally expressed in the platelet lineage[26]; therefore, we also performed a set of migration experiments in primary human MKs with DNM2 knockdown (Figure 2E; supplemental Figure 2C). Control and shDNM2 MK viabilities of were not significantly different (supplemental Figure 2D-E). A similar decrease in MKs was observed with DNM2 knockdown (Figure 2E), as with DNSR. We did not find a difference between control and shDNM3 MKs (supplemental Figure 2D). Altogether, using several approaches, we have established that directional migration of MKs is dependent on DNM activity.

DNM activity regulates actin polymerization, RhoA activation, and CXCR4 surface expression in human MKs

The actin cytoskeleton is the main constituent of MK migration. Because we observed that DNM inhibition leads to decreased MK migration, we studied its morphological effects on cytoskeleton

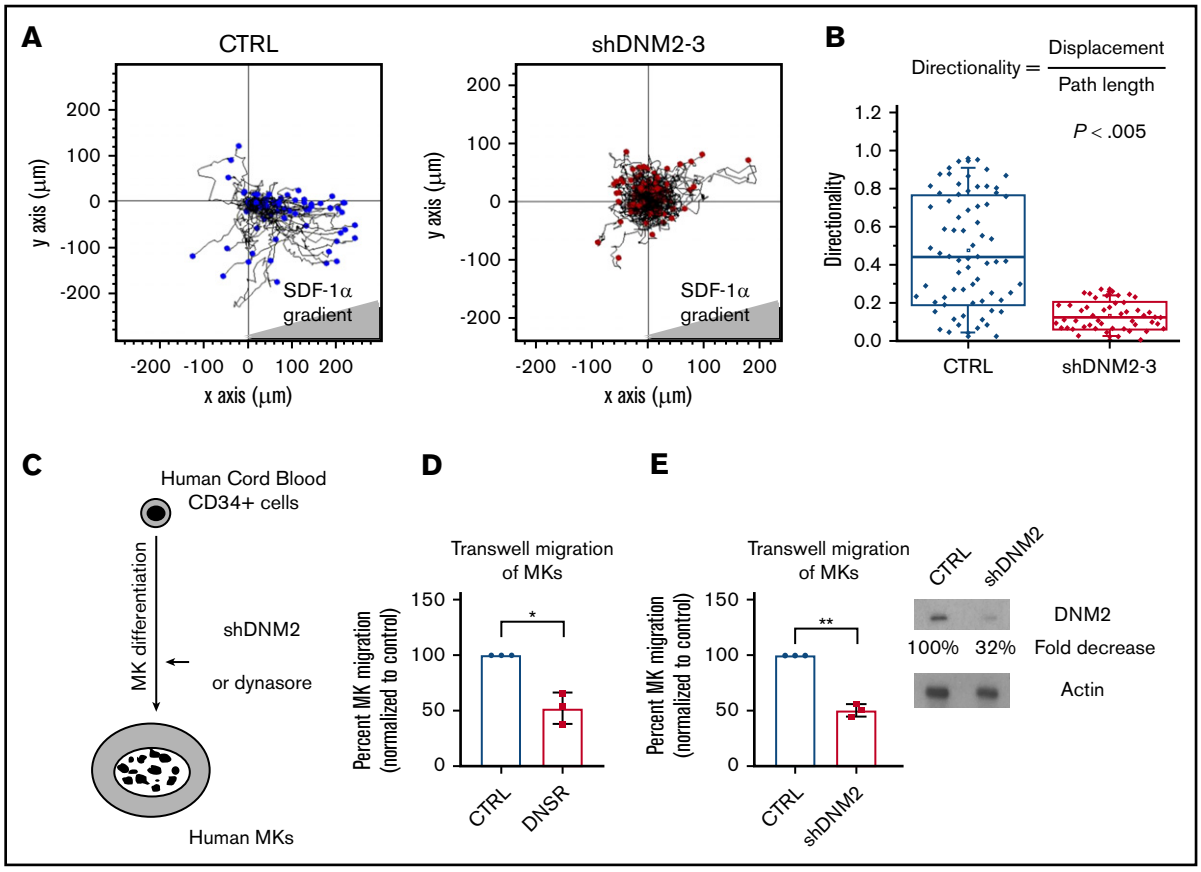

Figure 2. DNM activity is required for optimal MK migration. (A) Migration patterns of tracked CHRF cells without or with DNM knockdown on FN toward an SDF-1α gradient in the microfluidics-based μ-slide chemotaxis assay. (B) Quantification of directional migration of CHRF cells. ShDNM2 and shDNM3 CHRF cells exhibited a reduced directional migration toward an SDF-1α gradient ($P < .005$). (C) Schematic representation of the treatment of $CD34^+$ cell-derived human primary MKs. Before transwell migration assays, we differentiated human primary MKs from cord blood $CD34^+$ cells, which we would treat with shDNM2 or DNSR. (D) Quantification of MK migration in transwells toward a chemoattractant (SDF-1α) gradient, with the effect of DNSR. Migration was decreased by ~45% in DNSR-treated MKs vs control (CTRL; paired Student *t* test $P < .001$). (E) Quantification of MK migration in transwells toward a chemoattractant (SDF-1α) gradient, with the effect of DNM2 knockdown. Migration was decreased by approximately half in shDNM2-treated MKs vs CTRL (paired Student *t* test $P < .01$). Error bars indicate standard errors of the mean of ≥3 independent experiments. $^*P \leq .05$, $^{**}P \leq .01$.

rearrangement after adhesion on FN. By immunoconfocal imaging, DNSR-treated MKs showed disorganized, clumped F-actin, as opposed to the thinner mesh and the more even F-actin distribution within control cells (Figure 3A; supplemental Figure 3A).

We next assayed whole-cell F-actin polymerization in DNSR-treated MKs by flow cytometry. DNSR treatment of MKs decreased global actin polymerization by 25% compared with control MKs (Figure 3B-C). In parallel, we confirmed the findings in a cell line model; CHRF cells with shDNM2 or double shDNM2 and shDNM3 knockdown showed an ~25% decrease in actin polymerization (Figure 3D-E). A similar trend was noted in shDNM3 CHRF cells. Thus, by flow cytometry, we confirmed the impaired actin polymerization resulted from loss of DNM GTPase activity, because DNSR acts via DNM GTPase inhibition.

Because the small GTPase Rho regulates actin cytoskeleton rearrangement,[40] we next measured RhoA activity. The G-LISA method measures RhoA activation status by detecting the GTP-bound activated form of RhoA, which binds a Rho GTP-binding protein linked to the wells. GTP RhoA is then recognized by a RhoA antibody and measured by absorbance at 490 nm. RhoA activation was reduced by half in DNSR-treated MKs plated on FN (Figure 3F). Therefore, RhoA is a possible intermediate between upstream DNM activity and downstream actin cytoskeleton rearrangements. In contrast, we did not find significant differences in activated Rac or Cdc42 in DNSR-treated MKs compared with control (supplemental Figure 3B-C). The effect of DNM inhibition on various members of the Rho GTPase family, using different experimental conditions, should be the subject of future studies.

A CXCR4-Rho axis has previously been reported to mediate CXCR4-induced directional migration.[44] Because migration was altered in response to SDF-1α, we studied the expression of CXCR4, the G-protein–coupled receptor (GPCR) for SDF-1α. Cell surface expression of CXCR4 was modestly but significantly increased compared with control in MKs after treatment with DNSR (Figure 3G-H). The proportion of cells expressing CXCR4 was not significantly different between control and DNSR-treated MKs (supplemental Figure 3D). We reasoned that this might result from reduced endocytosis and might correlate with decreased CXCR4 activity. Indeed, we found a decreased change in staining

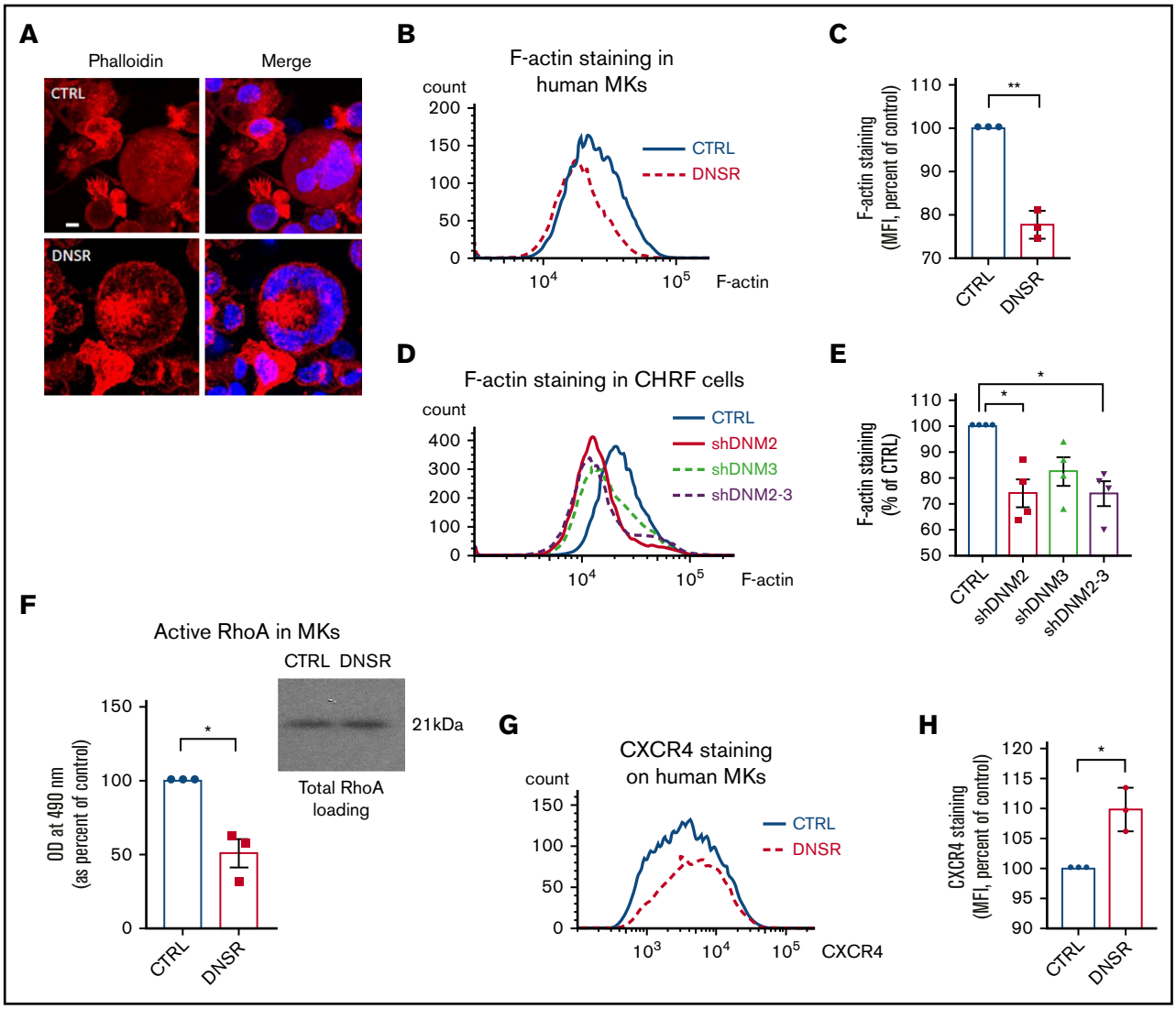

Figure 3. DNMs regulate actin cytoskeleton polymerization, RhoA activation, and surface CXCR4 expression in human MKs. (A) Distribution of F-actin in MKs of vehicle-treated control (CTRL) and DNSR-treated MKs plated on FN and stained with phalloidin (red) and DAPI (blue), without and with DNSR treatment. Twenty-five or more primary MKs were analyzed by confocal immunofluorescence. Here shown are OMX super-resolution microscopy images for illustration purposes. DNSR-treated MKs showed more unevenly distributed, disorganized, and clumped F-actin (arrow) compared with CTRL cells; original magnification, 63× objective. Scale bar represents 2 μm. (B-C) F-actin polymerization in MKs without and with DNSR treatment. Flow cytometry representative histograms and quantification in 3 experiments using fluorophore-conjugated phalloidin staining in permeabilized and fixed MKs. Actin polymerization was decreased by ~25% in DNSR-treated primary MKs (paired Student *t* test $P \leq .01$). (D-E) F-actin polymerization in CHRF cells without and with DNM knockdown. Flow cytometry representative histograms and quantification in 4 experiments using fluorophore-conjugated phalloidin staining in permeabilized and fixed CHRF cells. CHRF with shDNM2 or double knockdown for DNM2 and DNM3 showed an ~25% decrease in actin polymerization when compared with CTRL cells ($P < .05$). A similar trend was observed for CHRF cells with single shDNM3 knockdown. (F) RhoA activation quantification by G-LISA in MKs on FN. RhoA activation was reduced by half in DNSR-treated MKs (paired Student *t* test $P < .05$). (G-H) Surface CXCR4 expression in MKs. Flow cytometry representative histograms and quantification in 3 experiments. By flow cytometry, surface CXCR4 was slightly increased in DNSR-treated MKs (paired Student *t* test $P < .05$). Error bars indicate standard errors of the mean of ≥3 independent experiments. *$P \leq .05$, **$P \leq .01$. MFI, mean fluorescence intensity; OD, optical density.

intensity within the internalized CXCR4 fraction after SDF-1α treatment, using Imagestream imaging (supplemental Figure 3E).

Inhibition of endocytosis can block signaling downstream of GPCRs.[45] CXCR4 activity is indeed regulated by endocytosis and recycling.[46,47] Furthermore, CXCR4 recycling is dependent on Rho in human T cells.[48] Although the mechanisms for regulating CXCR4 activity remain a focus of active investigations[49] and experimental determination of CXCR4 activation state relies on indirect outcomes, our data suggest that the increased surface expression of CXCR4 reflects the loss of endocytosis, potentially leading to less active CXCR4 recycling toward the cell pole during chemotaxis and to loss of endosome-based signaling.[50]

DNMs regulate surface integrins in MKs

Because we assayed migration on FN, we chose to study the effect of DNMs on ITGB1, the main FN-interacting integrin. Moreover,

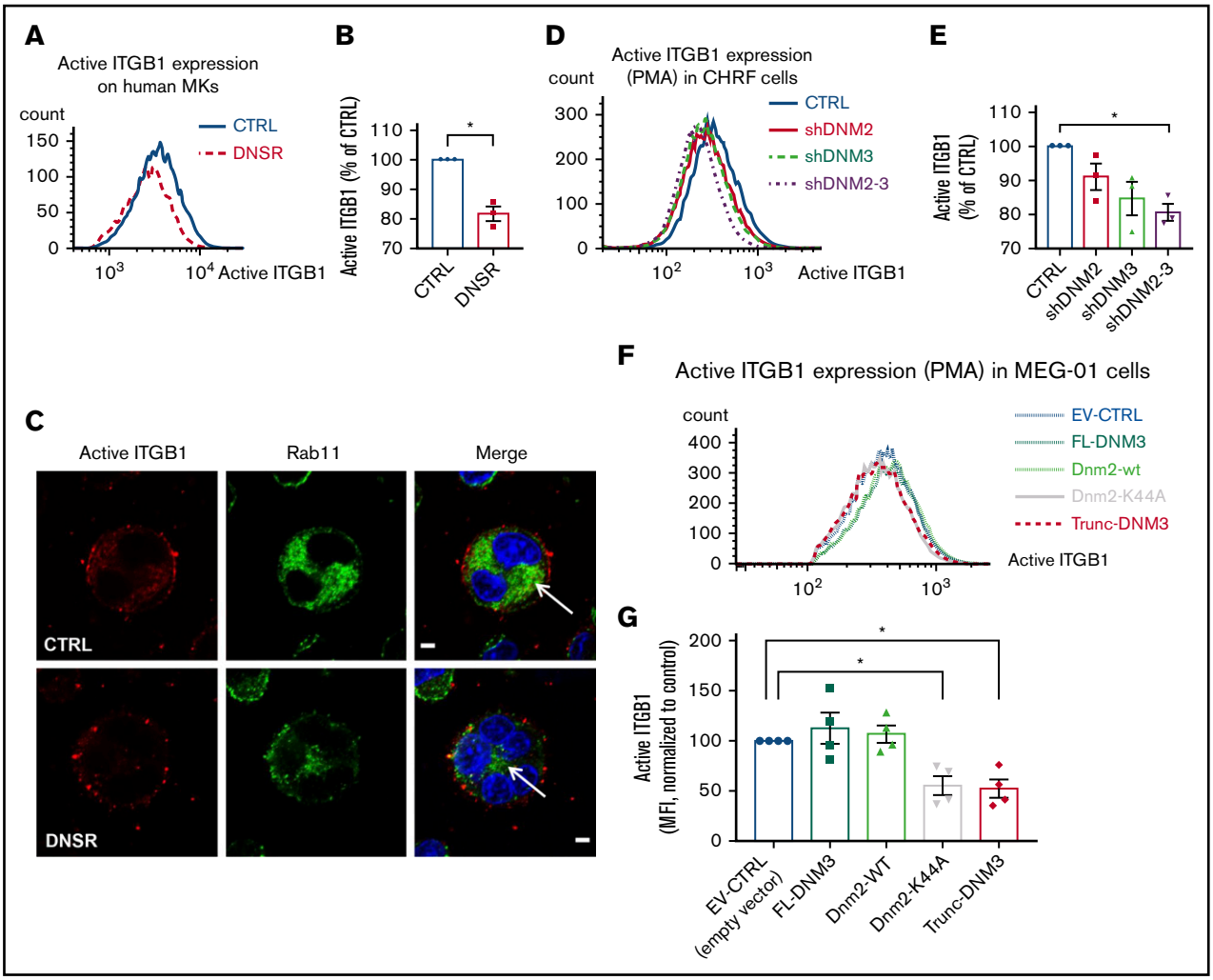

Figure 4. DNM inhibition affects ITGB1 activity and Rab11 cell distribution in human MKs. (A-B) Quantification of active ITGB1 at the surface of MKs. Representative flow cytometry histograms (A) and flow cytometry quantification (B) in 3 experiments measuring active ITGB1 at the surface of MKs after 2 hours on FN. ITGB1 activation was decreased by 17% in DNSR-treated MKs, when compared with control (CTRL) cells (paired Student *t* test $P = .001$). (C) Rab11 staining distribution in MKs on FN. MKs were stained with an antibody directed against Rab11 (green), a marker of recycling endosomes, and against activated ITGB1 (red). The nucleus is stained in blue. In the MKs that had not spread, Rab11 staining was more centrally clustered (arrow) in DNSR-treated cells, suggesting a decreased recycling process when compared with CTRL cells. Twenty-five or more primary MKs were analyzed. Images taken by Nikon A1R+ confocal microscope; original magnification, 60× Plan-Apochromat oil immersion lens. Scale bars represent 5 μm. (D-E) Quantification of active ITGB1 at the surface of CHRF cells transduced with nontargeting control or with shRNAs against DNM2 and DNM3. Representative flow cytometry histograms and flow cytometry quantification in 3 experiments in CHRF cells, activated with PMA (1 μM) and stained with an antibody specific for active ITGB1. Active surface ITGB1 in CHRF cells with shDNM2 and shDNM3 knockdown was reduced down to levels of 80% of CTRL cells. (F-G) Quantification of active ITGB1 at the surface of MEG-01 cells transduced with empty vector or with wild-type rat Dnm2 or human DNM3 or with DNM mutants. Flow cytometry representative histograms and quantification in 4 experiments in MEG-01 cells, activated with PMA (1 μM) and stained with an antibody specific for active ITGB1. In MEG-01 cells transduced with dominant-negative Dnm2-K44A or with truncated GTPase-less DNM3, active ITGB1 was reduced when compared with CTRL cells. Error bars indicate standard errors of the mean of ≥3 independent experiments. *$P \leq .05$.

ITGB1 activation usually lies upstream of Rho activation.[51-55] Although total surface ITGB1 was unchanged (data not shown), we also measured active ITGB1 in response to FN exposure. DNSR treatment decreased active ITGB1 by 17% in MKs (Figure 4A-B). Depletion or functional inhibition of DNM decreases early endosomes that display Rab5 and EEA1.[27,56] Early endosome content then gets sorted toward Rab11-tagged recycling endosomes or toward lysosomes for degradation.[57] Recycling plays an important role in maintaining surface integrin activity.[56-61] However, little is known regarding the role of DNMs on recycling endosome trafficking. Therefore, we studied the distribution of Rab11, a marker of recycling endosomes. We observed that in MKs cultured on FN, Rab11 staining was more centrally clustered in the DNSR-treated cells that had not spread, suggesting a lack of recruitment of the recycling pathway (Figure 4C). This lack of recycling is consistent with the decreased ITGB1 activation in DNSR-treated cells.

In parallel, we measured active ITGB1 by flow cytometry in CHRF cells transduced with shRNAs against DNM isoforms or in MEG-01

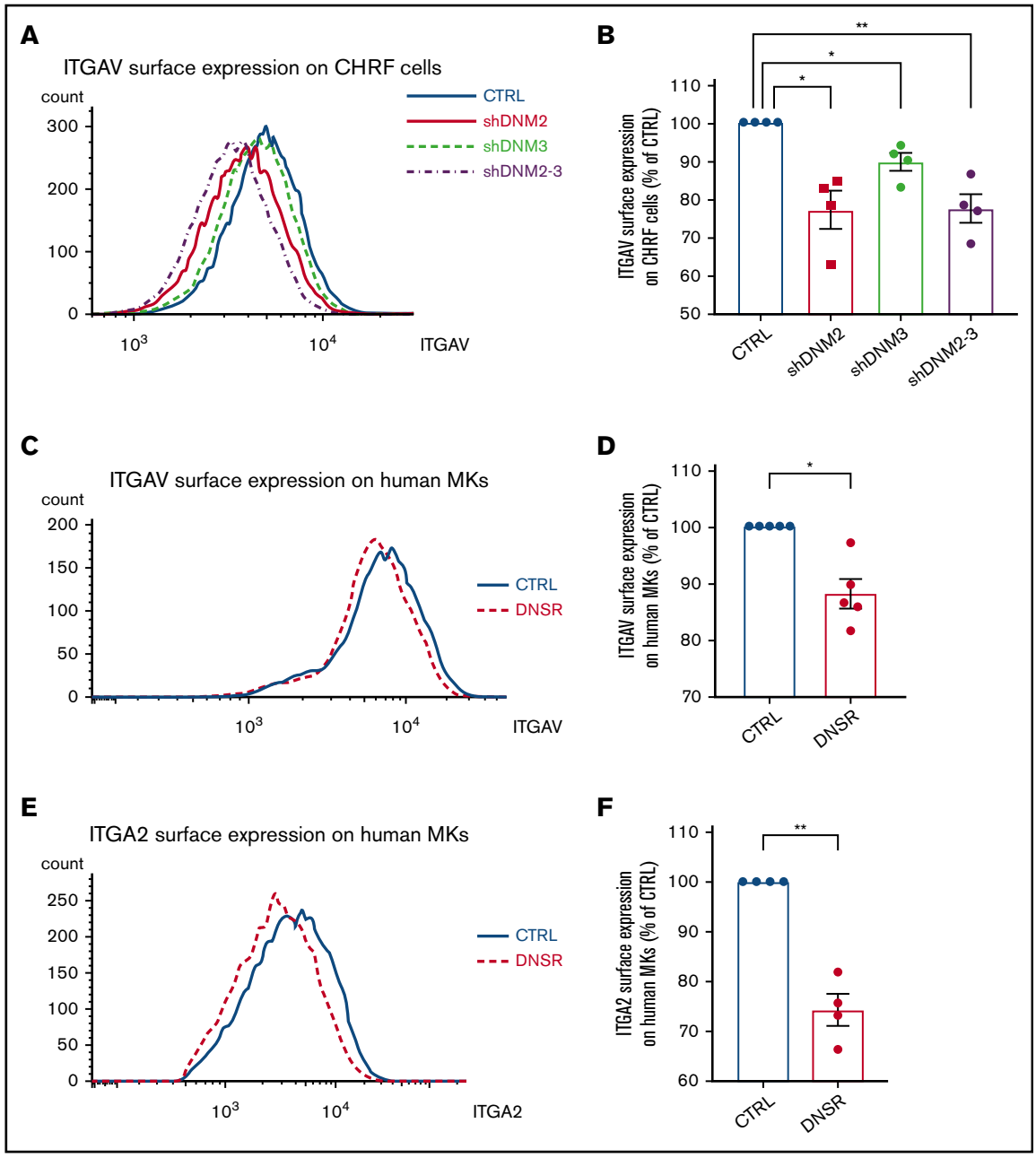

Figure 5. ITGA2 and ITGAV surface expression is affected by DNM activity in human MKs. (A-B) Quantification of ITGAV (part of a receptor to FN) at the surface of CHRF cells. Flow cytometry representative histograms and quantification in 4 experiments measuring ITGAV at the surface of CHRF cells. ITGAV staining shows a decrease in surface expression in CHRF with DNM2 and DNM3 knockdown when compared with control (CTRL; by 22%; paired Student *t* test $P < .05$). (C-D) Quantification of ITGAV at the surface of MKs. Flow cytometry representative histograms and quantification in 4 experiments measuring ITGAV at the surface of MKs. (E-F) ITGAV staining also showed a consistent slight decrease in primary MKs treated with DNSR (by 10%) when compared with control (paired Student *t* test $P < .05$). Quantification of ITGA2 at the surface of MKs. Flow cytometry representative histograms and quantification in 4 experiments measuring ITGA2 at the surface of MKs. ITGA2 staining (part of a receptor to collagen) showed a decrease in surface expression in primary MKs treated with DNSR (by 26% when compared with CTRL; paired Student *t* test $P < .05$). Error bars indicate standard errors of the mean of ≥3 independent experiments. *$P \leq .05$, **$P \leq .01$.

cells overexpressing rat Dnm2 and human DNM3 mutants. Both cell lines were treated with PMA to induce activation. Whereas total ITGB1 staining showed no difference across samples (data not shown), a decrease of active ITGB1 was observed in the CHRF cells transduced with shRNAs against both DNM isoforms (Figure 4D-E). Reduced ITGB1 activation was also seen in MEG-01 cells transduced with dominant-negative Dnm2-K44A or with truncated GTPase-deficient DNM3 (Figure 4F-G). Thus, we confirmed in 3 different models that DNM activity controls ITGB1 activity in megakaryocytic cells. In addition to abnormal CXCR4

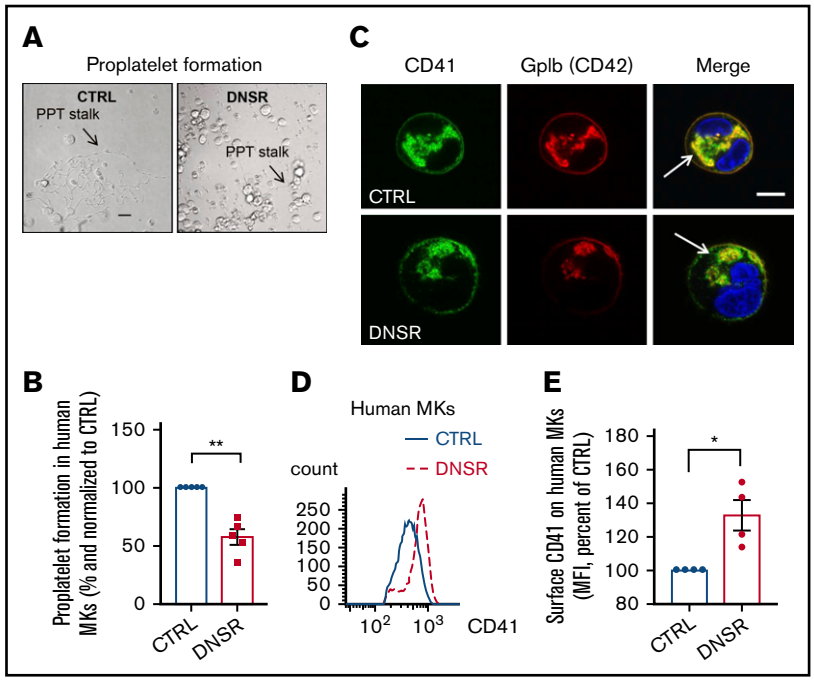

Figure 6. DNM activity is required for optimal PPF and adequate demarcation membrane system (DMS) development. (A-B) PPF representative fields on microscopy imaging and proplatelet (PPT) quantification. PPT stalks are shown with arrow. DNSR-treated MKs had reduced PPF by almost half (paired Student *t* test $P \leq .01$). Images taken by a Nikon Eclipse TS100 (×40 objective) and INFINITY capture camera and software (Luminera), analyzed with INFINITY Analyze software (Luminera). Scale bar represents 100 μm. (C) Gplb (CD42; red) staining of MK plasma membrane and intracellular DMS. Clumps, clustering, and uneven distribution of the DMS were observed within DNSR-treated MKs when compared with control (CTRL) MKs (arrows; supplemental Videos 3 and 4). The CD41 staining (green) showed the same trend of poor distribution within DNSR-treated MKs when compared with CTRL MKs. The nucleus is stained in blue. Images taken by Nikon A1R+ confocal microscope under a 60× Plan-Apochromat oil immersion lens. Scale bar represents 5 μm. (D-E) Representative flow cytometry histograms and flow cytometry quantification of CD41 at the surface of MKs. DNSR-treated MKs showed increased surface expression of CD41 (by 25%; paired Student *t* test $P < .05$). Error bars indicate standard errors of the mean of ≥3 independent experiments. *$P \leq .05$, **$P \leq .01$.

surface expression, reduced ITGB1 activity helps explain the defective directional migration in DNSR-treated MKs, upstream of the RhoA-actin cytoskeleton axis. Furthermore, we observed a dominant-negative effect for a GTPase-deficient DNM3 isoform, the existence of which is predicted by the alternate DNM3 transcript described previously[23,24] and demonstrated at the protein level by our western blot (Figure 1C). The dominant-negative effect of the GTPase-deficient DNM3 isoform might account for the lesser effect of the shDNM3 on cell behaviors when compared with shDNM2.

Surface expression of ITGA2 and ITGAV, partners of ITGB1, is affected by DNM activity

Because integrin activity is regulated at the level of the receptor complex,[52,62,63] we studied the effect of DNM inhibition on the α partners of the β1 integrin chains ITGAV (for the FN receptor) and ITGA2 (for the collagen receptor).[64] ITGAV was consistently decreased at the surface of CHRF cells with DNM isoform knockdown (Figure 5A-B) and slightly decreased on DNSR-treated MKs (Figure 5C-D). ITGA2 surface expression was also decreased in DNSR-treated MKs (Figure 5E-F). No change for ITGA5 was observed (data not shown). α Chains notably undergo endocytosis.[62] As discussed for active ITGB1, change in the α chain surface expression is consistent with defective recycling. As α chains regulate ITGB1 activity, their reduced expression is an additional mechanism for decreasing ITGB1 activity.[62] In summary, DNM inhibition alters the surface expression and activity of various membrane receptors. The extent of recycling impairment may differ among the active integrins.

DNM inhibition has extensive effects on membrane rearrangements, leading to perturbed PPF

As detailed in "DNM activity regulates actin polymerization, RhoA activation, and CXCR4 surface expression in human MKs" and "DNMs regulate surface integrins in MKs," cytoskeleton and integrin outcomes are affected by an inhibitor of endocytosis, and endocytosis is a particular case of membrane trafficking. Impairment of MK membrane remodeling capacity often manifests as abnormal PPF. MKs extend proplatelet protrusions, which are subsequently broken into preplatelets and platelets.[65-67] Indeed, we observed that PPF was reduced by half in DNSR-treated MKs (Figure 6A-B). The microtubules help PPF by protruding proplatelets from invaginated membrane reservoirs, called the DMS.[66-68] Because DNMs may interfere with microtubule dynamics,[19] we analyzed microtubule distribution in DNSR-treated MKs and controls. However, no striking difference was observed (data not shown). We then assessed the DMS by CD42 (Gp1b) staining of MK membranes.[69] CD41 (α2b), which pairs with CD61 (β3) to form the fibrinogen receptor, is also abundantly expressed at MK membranes. To visualize the external and invaginated internal membrane, CD41 and CD42 staining was performed for immunoconfocal analysis. Both CD41 and CD42 were less evenly distributed within DNSR-treated

MKs, compared with controls, forming internal clumps (Figure 6C; supplemental Videos 3 and 4). This finding is in agreement with a cell line model where knockdown of DNM3 impairs DMS-like structures[41] and with an animal model showing aberrant DMS development in murine MKs deficient for Dnm2.[27] DNSR-treated MKs displayed increased surface expression of CD41 (Figure 6D-E), most likely because of decreased endocytosis. Surface expression of CD42 was unchanged (data not shown), which was surprising given that both surface CD42 and CD61 are increased in murine platelets with Dnm2 knockout.[27] Together, these results suggest that DNM inhibition leads to defective PPF as a result of abnormal DMS development, emphasizing an additional important role for DNM-mediated selective endocytosis in MK.

Discussion

Here we report impaired directional migration in a human MK cell line with DNM2 and DNM3 knockdown and in primary human MKs treated with a small-molecule inhibitor of DNMs. We observed that impaired DNM activity affects actin filaments, which were disorganized into clumps and patches. As a result, this abnormality could disturb MK migration. The observed disorganization of polymerized actin was similar to that in murine pancreatic cells with *Dnm2* knockout.[20] Potential mechanisms include a direct effect of DNM on actin filament polymerization[70] or an indirect effect via the endocytosis and trafficking of cell surface receptors.

In MKs, RhoA lies at a crossroads as a major regulator of both actin cytoskeleton and PPF.[40,71,72] It was suggested that MK migration capacities are not crucial in some cases, such as steady-state thrombopoiesis or during recovery after short-term anti-Gp1b antibody–induced thrombocytopenia, because in these situations, a majority of MKs already reside close to the marrow sinusoids.[73] In another scenario, a total lack of migration toward hematopoietic organs had been described in the case of *ITGB1* deletion.[35] It is thus possible that migratory capacities are important for recovery after profound sustained cytopenia, where more immature progenitors are summoned, such as postchemotherapy or postirradiation states, as suggested by previous studies,[74] but not as crucial after short-term induced cytopenias, where late MK markers (Gp1b) are targeted.[73] Farther upstream of RhoA, DNMs modulate membrane receptor trafficking.[32] Indeed, we observed an increase in surface CXCR4 expression, as previously reported in T cells with *Dnm2* knockout,[75] presumably because of reduced endocytosis. Also, focal adhesion integrins, which link cells and the extracellular matrix,[76] undergo turnover under the control of DNM-based endocytosis.[77-79] Endocytosis is indeed the first step of integrin recycling. In a study on fibroblasts, sustaining ITGB1 activity was found to be dependent on initial endocytosis via DNM, followed by intracellular trafficking along the Rab11-recycling pathway.[60] In other studies, DNMs reportedly controlled the membrane exchange between intracellular compartments via Rab11-endosome pools.[80,81] Our observation of abnormally distributed Rab11 and decreased active ITGB1 in DNSR-treated MKs is supportive of the same phenomena taking place in MKs.[60] Other Rab proteins have been involved in platelet production.[82-86] Because Rab11 is present in platelets[61] and in MKs (our observation), it would be interesting to study the clinical relevance of Rab11 in hemostasis.

ITGB1 functions in dimers with α unit partners. In the MK lineage, the reduced surface ITGA2 observed in DNSR-treated cells will likely cause diminished podosome formation on collagen,[64,87] an additional potential way of impairing platelet biogenesis.[88] Roles for other receptors such as GPVI and DDR1 in MK motility and/or maturation have been previously reported by others.[11,89] Integrins modulate the activities of one another,[9,90] underscoring the complexity of MK-matrix interaction.

We propose a model (visual abstract) in which DNMs play a central role in MKs to control platelet output: at the cellular level, DNM activity regulates signaling pathways downstream of CXCR4 and integrins to trigger membrane-cytoskeleton rearrangements, and on a regional scale, DNMs regulate migration toward SDF-1α production sources, such as CAR (CXCL12-abundant reticular) cells in the vascular niche, where MKs initiate proplatelet production.

Additionally, we have gained novel information at the molecular level for guiding drug design. First, by using shRNAs to suppress each isoform DNM2 and DNM3 in a cell line model, we observed that both isoforms need to be targeted for maximal effect. Second, because findings in the shDNM2/shDNM3 cell line were also observed in MKs treated with GTPase inhibitor DNSR, we clarified the specific effects of DNM GTPase activity vs other DNM properties, such as scaffolding.[19,91] Our study identifies the importance of DNMs in affecting MK migration during megakaryopoiesis and provides a new target for platelet production.

Acknowledgments

The authors thank William Vainchenker, Andrew Volk, and Maureen McNulty for critical review of the manuscript; Pietro de Camilli, William Miller, Richard Minshall, and François Lanza for providing reagents; Jorie Aardema and Hrishikesh Mehta for help with the molecular biology; Usua Oyarbide for help with the cell culture; Joshua Rappoport, Constadina Arvanitis, David Kirchenbuechler, Peter Dluhy, and Wensheng (Wilson) Liu for help with confocal imaging; Thomas J. Hope and João I. Mamede for help with the DeltaVision-OMX super-resolution microscope; Suchitra Swaminathan for help with flow cytometry analysis; Paul Mehl for fluorescence-activated cell sorting; and David Leclerc, Brian Hall, and Robert Thacker for assistance in Imagestream experiments.

This work was supported by grants from the American Heart Association Post-Doctoral Fellowship (12POST9530010) and National Institutes of Health (NIH), National, Heart, Lung, and Blood Institute grants K08 HL114871 (Y.C.), RO1 HL080052 and R21 HL106462 (S.J.C.), and RO1 HL112792 (J.D.C.); the American Heart Association Grant-in-Aid (S.J.C.); NIH, National Cancer Institute grant T32CA080621 (S.H.); NIH, National Institute of Diabetes and Digestive and Kidney Diseases grant RO1 DK098812 (E.A.E.); and the Ligue Nationale Contre le Cancer Equipe labellisée 2016-2018 (N.D.). R.I. was supported by a fellowship from the Higher Education Commission, Pakistan. The Northwestern University Flow Cytometry Core Facility was supported by NIH, National Cancer Insistute Cancer Center Support Grant CA060553. Flow Cytometry Cell Sorting was performed on a BD FACSAria SORP system, purchased through the support of NIH Office of the Director Award 1S10OD011996-01.

Authorship

Contribution: P.K.S., S.J.C., M.J.H., R.I., A.A., S.H., C.S., N.D., J.D.C., E.A.E., and Y.C. designed experiments, performed research and/or analyzed data, and wrote the manuscript; J.D.C., E.A.E., A.W., and

H.L. provided critical materials and reagents; and P.K.S., S.J.C., M.J.H., S.H., N.D., J.D.C., E.A.E., and Y.C. wrote the manuscript.

Conflict-of-interest disclosure: C.S. is an employee of MilliporeSigma. The remaining authors declare no competing financial interests.

The current affiliation for S.J.C. is Department of Pediatrics and Molecular Medicine, Cleveland Clinic, Cleveland, OH.

Correspondence: Yolande Chen, Department of Medicine, Hematology/Oncology, Northwestern University School of Medicine, Lurie Building, 5th floor, 303 E. Superior St, Chicago IL 60611; e-mail: yolande-chen@northwestern.edu; and Seth J. Corey, Department of Pediatrics and Molecular Medicine, Box R3, Cleveland Clinic, 9500 Euclid Ave, Cleveland, OH 44195; e-mail: coreylab@yahoo.com.

References

1. Wang JF, Liu ZY, Groopman JE. The alpha-chemokine receptor CXCR4 is expressed on the megakaryocytic lineage from progenitor to platelets and modulates migration and adhesion. *Blood*. 1998;92(3):756-764.
2. Hamada T, Möhle R, Hesselgesser J, et al. Transendothelial migration of megakaryocytes in response to stromal cell-derived factor 1 (SDF-1) enhances platelet formation. *J Exp Med*. 1998;188(3):539-548.
3. Rivière C, Subra F, Cohen-Solal K, et al. Phenotypic and functional evidence for the expression of CXCR4 receptor during megakaryocytopoiesis. *Blood*. 1999;93(5):1511-1523.
4. Drayer AL, Sibinga CT, Blom NR, De Wolf JT, Vellenga E. The in vitro effects of cytokines on expansion and migration of megakaryocyte progenitors. *Br J Haematol*. 2000;109(4):776-784.
5. Dias S, Hattori K, Zhu Z, et al. Autocrine stimulation of VEGFR-2 activates human leukemic cell growth and migration. *J Clin Invest*. 2000;106(4):511-521.
6. Avecilla ST, Hattori K, Heissig B, et al. Chemokine-mediated interaction of hematopoietic progenitors with the bone marrow vascular niche is required for thrombopoiesis. *Nat Med*. 2004;10(1):64-71.
7. Gilles L, Bluteau D, Boukour S, et al. MAL/SRF complex is involved in platelet formation and megakaryocyte migration by regulating MYL9 (MLC2) and MMP9. *Blood*. 2009;114(19):4221-4232.
8. Ragu C, Elain G, Mylonas E, et al. The transcription factor Srf regulates hematopoietic stem cell adhesion. *Blood*. 2010;116(22):4464-4473.
9. Mazharian A, Thomas SG, Dhanjal TS, Buckley CD, Watson SP. Critical role of Src-Syk-PLCgamma2 signaling in megakaryocyte migration and thrombopoiesis. *Blood*. 2010;116(5):793-800.
10. Mazharian A. Assessment of megakaryocyte migration and chemotaxis. *Methods Mol Biol*. 2012;788:275-288.
11. Abbonante V, Gruppi C, Rubel D, Gross O, Moratti R, Balduini A. Discoidin domain receptor 1 protein is a novel modulator of megakaryocyte-collagen interactions. *J Biol Chem*. 2013;288(23):16738-16746.
12. Malara A, Gruppi C, Pallotta I, et al. Extracellular matrix structure and nano-mechanics determine megakaryocyte function. *Blood*. 2011;118(16):4449-4453.
13. Eliades A, Papadantonakis N, Bhupatiraju A, et al. Control of megakaryocyte expansion and bone marrow fibrosis by lysyl oxidase. *J Biol Chem*. 2011;286(31):27630-27638.
14. Leiva O, Leon C, Kah Ng S, Mangin P, Gachet C, Ravid K. The role of extracellular matrix stiffness in megakaryocyte and platelet development and function. *Am J Hematol*. 2018;93(3):430-441.
15. Desterke C, Martinaud C, Guerton B, et al. Tetraspanin CD9 participates in dysmegakaryopoiesis and stromal interactions in primary myelofibrosis. *Haematologica*. 2015;100(6):757-767.
16. Lane WJ, Dias S, Hattori K, et al. Stromal-derived factor 1-induced megakaryocyte migration and platelet production is dependent on matrix metalloproteinases. *Blood*. 2000;96(13):4152-4159.
17. Kowalska MA, Ratajczak J, Hoxie J, et al. Megakaryocyte precursors, megakaryocytes and platelets express the HIV co-receptor CXCR4 on their surface: determination of response to stromal-derived factor-1 by megakaryocytes and platelets. *Br J Haematol*. 1999;104(2):220-229.
18. Chen Y, Aardema J, Kale S, et al. Loss of the F-BAR protein CIP4 reduces platelet production by impairing membrane-cytoskeleton remodeling. *Blood*. 2013;122(10):1695-1706.
19. Ferguson SM, De Camilli P. Dynamin, a membrane-remodelling GTPase. *Nat Rev Mol Cell Biol*. 2012;13(2):75-88.
20. Fan F, Ji C, Wu Y, et al. Dynamin 2 regulates biphasic insulin secretion and plasma glucose homeostasis. *J Clin Invest*. 2015;125(11):4026-4041.
21. Reems JA, Wang W, Tsubata K, et al. Dynamin 3 participates in the growth and development of megakaryocytes. *Exp Hematol*. 2008;36(12):1714-1727.
22. Claeys KG, Züchner S, Kennerson M, et al. Phenotypic spectrum of dynamin 2 mutations in Charcot-Marie-Tooth neuropathy. *Brain*. 2009;132(Pt 7):1741-1752.
23. Soranzo N, Spector TD, Mangino M, et al. A genome-wide meta-analysis identifies 22 loci associated with eight hematological parameters in the HaemGen consortium. *Nat Genet*. 2009;41(11):1182-1190.
24. Nürnberg ST, Rendon A, Smethurst PA, et al; HaemGen Consortium. A GWAS sequence variant for platelet volume marks an alternative DNM3 promoter in megakaryocytes near a MEIS1 binding site. *Blood*. 2012;120(24):4859-4868.
25. Raimondi A, Ferguson SM, Lou X, et al. Overlapping role of dynamin isoforms in synaptic vesicle endocytosis. *Neuron*. 2011;70(6):1100-1114.

26. Rowley JW, Oler AJ, Tolley ND, et al. Genome-wide RNA-seq analysis of human and mouse platelet transcriptomes. *Blood*. 2011;118(14):e101-e111.
27. Bender M, Giannini S, Grozovsky R, et al. Dynamin 2-dependent endocytosis is required for normal megakaryocyte development in mice. *Blood*. 2015; 125(6):1014-1024.
28. Kruchten AE, McNiven MA. Dynamin as a mover and pincher during cell migration and invasion. *J Cell Sci*. 2006;119(Pt 9):1683-1690.
29. Eppinga RD, Krueger EW, Weller SG, Zhang L, Cao H, McNiven MA. Increased expression of the large GTPase dynamin 2 potentiates metastatic migration and invasion of pancreatic ductal carcinoma. *Oncogene*. 2012;31(10):1228-1241.
30. Feng H, Liu KW, Guo P, et al. Dynamin 2 mediates PDGFRα-SHP-2-promoted glioblastoma growth and invasion. *Oncogene*. 2012;31(21):2691-2702.
31. Razidlo GL, Wang Y, Chen J, Krueger EW, Billadeau DD, McNiven MA. Dynamin 2 potentiates invasive migration of pancreatic tumor cells through stabilization of the Rac1 GEF Vav1. *Dev Cell*. 2013;24(6):573-585.
32. Tremblay CS, Brown FC, Collett M, et al. Loss-of-function mutations of dynamin 2 promote T-ALL by enhancing IL-7 signalling. *Leukemia*. 2016;30(10): 1993-2001.
33. Krueger EW, Orth JD, Cao H, McNiven MA. A dynamin-cortactin-Arp2/3 complex mediates actin reorganization in growth factor-stimulated cells. *Mol Biol Cell*. 2003;14(3):1085-1096.
34. Schlunck G, Damke H, Kiosses WB, et al. Modulation of Rac localization and function by dynamin. *Mol Biol Cell*. 2004;15(1):256-267.
35. Fässler R, Meyer M. Consequences of lack of beta 1 integrin gene expression in mice. *Genes Dev*. 1995;9(15):1896-1908.
36. Futami M, Zhu QS, Whichard ZL, et al. G-CSF receptor activation of the Src kinase Lyn is mediated by Gab2 recruitment of the Shp2 phosphatase. *Blood*. 2011;118(4):1077-1086.
37. Suraneni P, Fogelson B, Rubinstein B, et al. A mechanism of leading-edge protrusion in the absence of Arp2/3 complex. *Mol Biol Cell*. 2015;26(5): 901-912.
38. Suraneni P, Rubinstein B, Unruh JR, Durnin M, Hanein D, Li R. The Arp2/3 complex is required for lamellipodia extension and directional fibroblast cell migration. *J Cell Biol*. 2012;197(2):239-251.
39. Berthebaud M, Rivière C, Jarrier P, et al. RGS16 is a negative regulator of SDF-1-CXCR4 signaling in megakaryocytes. *Blood*. 2005;106(9): 2962-2968.
40. Chang Y, Auradé F, Larbret F, et al. Proplatelet formation is regulated by the Rho/ROCK pathway. *Blood*. 2007;109(10):4229-4236.
41. Wang W, Gilligan DM, Sun S, Wu X, Reems JA. Distinct functional effects for dynamin3 during megakaryocytopoiesis. *Stem Cells Dev*. 2011;20(12): 2139-2151.
42. Dmitrieff S, Nédélec F. Membrane mechanics of endocytosis in cells with turgor. *PLOS Comput Biol*. 2015;11(10):e1004538.
43. Malara A, Gruppi C, Rebuzzini P, et al. Megakaryocyte-matrix interaction within bone marrow: new roles for fibronectin and factor XIII-A. *Blood*. 2011; 117(8):2476-2483.
44. Tan W, Martin D, Gutkind JS. The Galpha13-Rho signaling axis is required for SDF-1-induced migration through CXCR4. *J Biol Chem*. 2006;281(51): 39542-39549.
45. Zhang X, Kim KM. Multifactorial regulation of G protein-coupled receptor endocytosis. *Biomol Ther (Seoul)*. 2017;25(1):26-43.
46. Pelekanos RA, Ting MJ, Sardesai VS, et al. Intracellular trafficking and endocytosis of CXCR4 in fetal mesenchymal stem/stromal cells. *BMC Cell Biol*. 2014;15:15.
47. Bamidele AO, Kremer KN, Hirsova P, et al. IQGAP1 promotes CXCR4 chemokine receptor function and trafficking via EEA-1+ endosomes. *J Cell Biol*. 2015;210(2):257-272.
48. Kumar A, Kremer KN, Dominguez D, Tadi M, Hedin KE. Gα13 and Rho mediate endosomal trafficking of CXCR4 into Rab11+ vesicles upon stromal cell-derived factor-1 stimulation. *J Immunol*. 2011;186(2):951-958.
49. Wescott MP, Kufareva I, Paes C, et al. Signal transmission through the CXC chemokine receptor 4 (CXCR4) transmembrane helices. *Proc Natl Acad Sci USA*. 2016;113(35):9928-9933.
50. Hanyaloglu AC, von Zastrow M. Regulation of GPCRs by endocytic membrane trafficking and its potential implications. *Annu Rev Pharmacol Toxicol*. 2008;48:537-568.
51. Huveneers S, Danen EH. Adhesion signaling - crosstalk between integrins, Src and Rho. *J Cell Sci*. 2009;122(Pt 8):1059-1069.
52. Schiller HB, Hermann MR, Polleux J, et al. β1- and αv-class integrins cooperate to regulate myosin II during rigidity sensing of fibronectin-based microenvironments. *Nat Cell Biol*. 2013;15(6):625-636.
53. Shen B, Estevez B, Xu Z, et al. The interaction of Gα13 with integrin β1 mediates cell migration by dynamic regulation of RhoA. *Mol Biol Cell*. 2015; 26(20):3658-3670.
54. Calderwood DA. Integrin activation. *J Cell Sci*. 2004;117(Pt 5):657-666.
55. Moser M, Legate KR, Zent R, Fässler R. The tail of integrins, talin, and kindlins. *Science*. 2009;324(5929):895-899.
56. Alanko J, Mai A, Jacquemet G, et al. Integrin endosomal signalling suppresses anoikis. *Nat Cell Biol*. 2015;17(11):1412-1421.
57. Tiwari A, Jung JJ, Inamdar SM, Brown CO, Goel A, Choudhury A. Endothelial cell migration on fibronectin is regulated by syntaxin 6-mediated alpha5beta1 integrin recycling. *J Biol Chem*. 2011;286(42):36749-36761.
58. Fang Z, Takizawa N, Wilson KA, et al. The membrane-associated protein, supervillin, accelerates F-actin-dependent rapid integrin recycling and cell motility. *Traffic*. 2010;11(6):782-799.

59. De Franceschi N, Hamidi H, Alanko J, Sahgal P, Ivaska J. Integrin traffic - the update. *J Cell Sci*. 2015;128(5):839-852.

60. Nader GP, Ezratty EJ, Gundersen GG. FAK, talin and PIPKIγ regulate endocytosed integrin activation to polarize focal adhesion assembly. *Nat Cell Biol*. 2016;18(5):491-503.

61. Huang Y, Joshi S, Xiang B, et al. Arf6 controls platelet spreading and clot retraction via integrin αIIbβ3 trafficking. *Blood*. 2016;127(11):1459-1467.

62. Wang Z, Leisner TM, Parise LV. Platelet alpha2beta1 integrin activation: contribution of ligand internalization and the alpha2-cytoplasmic domain. *Blood*. 2003;102(4):1307-1315.

63. Rantala JK, Pouwels J, Pellinen T, et al. SHARPIN is an endogenous inhibitor of β1-integrin activation. *Nat Cell Biol*. 2011;13(11):1315-1324.

64. Sabri S, Jandrot-Perrus M, Bertoglio J, et al. Differential regulation of actin stress fiber assembly and proplatelet formation by alpha2beta1 integrin and GPVI in human megakaryocytes. *Blood*. 2004;104(10):3117-3125.

65. Junt T, Schulze H, Chen Z, et al. Dynamic visualization of thrombopoiesis within bone marrow. *Science*. 2007;317(5845):1767-1770.

66. Patel SR, Hartwig JH, Italiano JE Jr. The biogenesis of platelets from megakaryocyte proplatelets. *J Clin Invest*. 2005;115(12):3348-3354.

67. Machlus KR, Thon JN, Italiano JE Jr. Interpreting the developmental dance of the megakaryocyte: a review of the cellular and molecular processes mediating platelet formation. *Br J Haematol*. 2014;165(2):227-236.

68. Patel SR, Richardson JL, Schulze H, et al. Differential roles of microtubule assembly and sliding in proplatelet formation by megakaryocytes. *Blood*. 2005;106(13):4076-4085.

69. Eckly A, Heijnen H, Pertuy F, et al. Biogenesis of the demarcation membrane system (DMS) in megakaryocytes. *Blood*. 2014;123(6):921-930.

70. Gu C, Yaddanapudi S, Weins A, et al. Direct dynamin-actin interactions regulate the actin cytoskeleton. *EMBO J*. 2010;29(21):3593-3606.

71. Pleines I, Hagedorn I, Gupta S, et al. Megakaryocyte-specific RhoA deficiency causes macrothrombocytopenia and defective platelet activation in hemostasis and thrombosis. *Blood*. 2012;119(4):1054-1063.

72. Poggi M, Canault M, Favier M, et al. Germline variants in ETV6 underlie reduced platelet formation, platelet dysfunction and increased levels of circulating CD34+ progenitors. *Haematologica*. 2017;102(2):282-294.

73. Stegner D, vanEeuwijk JMM, Angay O, et al. Thrombopoiesis is spatially regulated by the bone marrow vasculature. *Nat Commun*. 2017;8(1):127.

74. Niswander LM, Fegan KH, Kingsley PD, McGrath KE, Palis J. SDF-1 dynamically mediates megakaryocyte niche occupancy and thrombopoiesis at steady state and following radiation injury. *Blood*. 2014;124(2):277-286.

75. Willinger T, Ferguson SM, Pereira JP, De Camilli P, Flavell RA. Dynamin 2-dependent endocytosis is required for sustained S1PR1 signaling. *J Exp Med*. 2014;211(4):685-700.

76. Etienne-Manneville S. Microtubules in cell migration. *Annu Rev Cell Dev Biol*. 2013;29(1):471-499.

77. Ezratty EJ, Partridge MA, Gundersen GG. Microtubule-induced focal adhesion disassembly is mediated by dynamin and focal adhesion kinase. *Nat Cell Biol*. 2005;7(6):581-590.

78. Chao WT, Kunz J. Focal adhesion disassembly requires clathrin-dependent endocytosis of integrins. *FEBS Lett*. 2009;583(8):1337-1343.

79. Chao WT, Ashcroft F, Daquinag AC, et al. Type I phosphatidylinositol phosphate kinase beta regulates focal adhesion disassembly by promoting beta1 integrin endocytosis. *Mol Cell Biol*. 2010;30(18):4463-4479.

80. Pelissier A, Chauvin JP, Lecuit T. Trafficking through Rab11 endosomes is required for cellularization during Drosophila embryogenesis. *Curr Biol*. 2003;13(21):1848-1857.

81. Takahashi Y, Tsotakos N, Liu Y, et al. The Bif-1-dynamin 2 membrane fission machinery regulates Atg9-containing vesicle generation at the Rab11-positive reservoirs. *Oncotarget*. 2016;7(15):20855-20868.

82. Stenmark H. Rab GTPases as coordinators of vesicle traffic. *Nat Rev Mol Cell Biol*. 2009;10(8):513-525.

83. Griscelli C, Durandy A, Guy-Grand D, Daguillard F, Herzog C, Prunieras M. A syndrome associating partial albinism and immunodeficiency. *Am J Med*. 1978;65(4):691-702.

84. Novak EK, Reddington M, Zhen L, et al. Inherited thrombocytopenia caused by reduced platelet production in mice with the gunmetal pigment gene mutation. *Blood*. 1995;85(7):1781-1789.

85. Barral DC, Ramalho JS, Anders R, et al. Functional redundancy of Rab27 proteins and the pathogenesis of Griscelli syndrome. *J Clin Invest*. 2002;110(2):247-257.

86. Tiwari S, Italiano JE Jr, Barral DC, et al. A role for Rab27b in NF-E2-dependent pathways of platelet formation. *Blood*. 2003;102(12):3970-3979.

87. Sabri S, Foudi A, Boukour S, et al. Deficiency in the Wiskott-Aldrich protein induces premature proplatelet formation and platelet production in the bone marrow compartment. *Blood*. 2006;108(1):134-140.

88. Schachtner H, Calaminus SD, Sinclair A, et al. Megakaryocytes assemble podosomes that degrade matrix and protrude through basement membrane. *Blood*. 2013;121(13):2542-2552.

89. Inoue O, Suzuki-Inoue K, McCarty OJ, et al. Laminin stimulates spreading of platelets through integrin alpha6beta1-dependent activation of GPVI. *Blood*. 2006;107(4):1405-1412.

90. Cruz MA, Chen J, Whitelock JL, Morales LD, López JA. The platelet glycoprotein Ib-von Willebrand factor interaction activates the collagen receptor alpha2beta1 to bind collagen: activation-dependent conformational change of the alpha2-I domain. *Blood*. 2005;105(5):1986-1991.

91. McNiven MA, Kim L, Krueger EW, Orth JD, Cao H, Wong TW. Regulated interactions between dynamin and the actin-binding protein cortactin modulate cell shape. *J Cell Biol*. 2000;151(1):187-198.